



Shape Information of Curves and its Visualization using Two-tone Pseudo Coloring

Norimasa Yoshida¹ , Takafumi Saito² 

¹Nihon University, yoshida.norimasa@nihon-u.ac.jp

²Tokyo University of Agriculture and Technology, txsaito@cc.tuat.ac.jp

Corresponding author: Norimasa Yoshida, yoshida.norimasa@nihon-u.ac.jp

Abstract. This paper presents a method for computing and visualizing the shape information of differentiable parametric curves. The shape information is the slope α of the logarithmic curvature graph and the slope β of the logarithmic torsion graph. We derive the equations for computing α and β in terms of curvature and torsion, respectively. The value of α is related to the specific curvature function, such as the linear function when $\alpha = -1$. For space curves, the value of β is also related to the specific torsion function. Using the two-tone pseudo coloring for the visualization of the shape information, users can read out the approximate value of α and β for each point of the curve. For some planar curves, we clarify the similarities with log-aesthetic curves by taking the limit of α as the parameter approaches the limit value.

Keywords: logarithmic curvature graph, logarithmic torsion graph, shape information, log-aesthetic curves, two-tone pseudo coloring

DOI: <https://doi.org/10.14733/cadaps.2024.11-28>

1 INTRODUCTION

To design aesthetic objects in industrial or conceptual design, inspecting the geometric quality of curves and surfaces is inevitable. Since the geometric quality is not easy to grasp from their rendered image, CAD systems are usually equipped with special tools. Such inspection tools for surfaces include reflections lines [8], isophotoes [10], or color map of Gaussian or mean curvature [1].

Curvature plots and curvature combs [4] are widely used in CAD systems for obtaining information about curvature. Using these tools, designers can recognize regions of monotone curvature and check if curvature extrema occur at points intended by the designers [2]. These tools are especially important for designing aesthetic objects in industrial or conceptual design since such objects are usually based on an initial set of fair curves.

To examine the shape information of a curve that cannot be easily obtained by curvature plots or curvature combs, logarithmic curvature graphs (LCGs) have been proposed [13]. For space curves, logarithmic torsion

graphs (LTGs) have been also proposed. The slope of the LCG or LTG is called α or β , respectively. For a planar curve, if its LCG is close to be linear with its slope α , it means the curve is close to the log-aesthetic curve [14, 16] with the shape parameter α . Similarly, for space curves, if its LCG and LTG are close to be linear with their slopes α and β , respectively, the curve is close to the log-aesthetic space curve [12] with the shape parameter α and β . LCGs and LTGs are good for checking the linearity, but they both have a problem that it is not easy to know which point of a curve corresponds to which point in the LCG or LTG.

The contributions of this work are the following.

- Equations for computing α (and β for space curves) for each point of a parametric curve segment
The equation for α in terms of the radius of curvature is presented in [5]. We derive the equation in terms of curvature and describe the details, such as the case when κ or $\frac{d\kappa}{ds}$ is negative.
- Visualization of the shape information (α and β) using two-tone pseudo coloring
By using the two-tone pseudo coloring[11], users can read out the approximate value of α (and β). For example, if the color of a curve segment is almost red, it means the curve is close to the log-aesthetic curve with $\alpha = 1$, which is a logarithmic spiral. Using the two-tone pseudo coloring, users can read out the approximate value of α (and β) for each point of a curve segment if the value is within a specified range. If the color changes from red to orange, it means the curve is changing from a logarithmic spiral ($\alpha = 1$) to the circle involute ($\alpha = 2$). Since α is visualized with respect to the arc length, users can also recognize the speed of change.
- Clarifying the shape similarities of some planar curves in differential geometry with log-aesthetic curves
For some planar curves, we clarify the shape similarities with log-aesthetic curves regarding the LCG slope α . For example, the hyperbola gets closer to the log-aesthetic curve with $\alpha = \frac{1}{3}$ as the parameter approaches $\pm\infty$.

The paper is organized as follows. Section 2 reviews LCGs, LTGs, and their properties. Section 3 derives the equations for α and β and describes the detailed situations where the slopes are defined. Section 4 proposes a method for visualizing the shape information using two-tone pseudo coloring and shows examples of visualizing polynomial and rational Bézier curves. Section 5 analyzes some planar parametric curves through the LCG slopes and clarifies similarities with log-aesthetic curves. Finally, conclusions are presented in Section 6.

2 LOGARITHMIC CURVATURE AND TORSION GRAPHS

This section reviews the logarithmic curvature graph (LCGs) and logarithmic torsion graphs (LTGs) [13] and their properties. Originally, logarithmic curvature graphs are formulated by the radius of curvature [7, 9, 14]. In this paper, we use the formulation by curvature [13]. Curves with linear LCGs are called *log-aesthetic curves* [14, 16]. If both the LCG and LTG are linear, the curve is called *log-aesthetic space curves* [12]. *Quadratic log-aesthetic curves* whose LCGs are quadratic are investigated in [15]. In this section, we assume that the curvature is monotonically increasing as the arc length increases. In previous work [14, 13], the radius of curvature is assumed to be monotonically increasing. Therefore, the equations in this section are slightly different from equations in [13].

Let κ and s be the curvature and the arc length, respectively. The linearity of LCG is

$$\log\left(\kappa\frac{ds}{d\kappa}\right) = -\alpha\log\kappa + c, \quad (1)$$

where α is the slope and c is a constant. “−” before “ $\alpha\log\kappa$ ” is necessary for the value of α to have the same meaning as the formulation by the radius of curvature. If κ or $\frac{ds}{d\kappa}$ takes a negative value, its absolute value

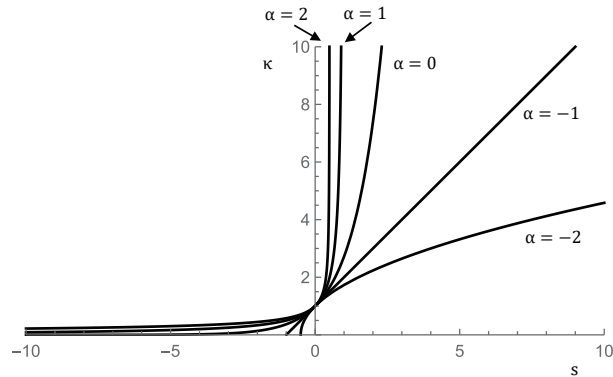


Figure 1: Curvature plot of log-aesthetic curves ($\Lambda = 1$).

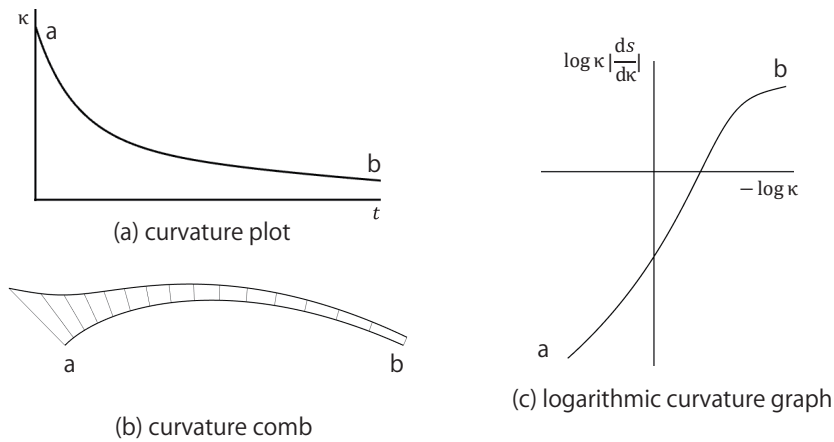


Figure 2: Cubic Bézier curve with monotonically varying curvature.

is taken. The linearity of the LCG is especially important because the curve becomes the Clothoid, Nielsen’s spiral, a logarithmic spiral or the circle involute when $\alpha = -1, 0, 1$ or 2 , respectively. Modifying Eq. (1) and setting $\Lambda = e^{-c}$, we get the following curvature function in the standard form ($\kappa = 1$ at $s = 0$):

$$\kappa = \begin{cases} e^{\Lambda s} & \text{if } \alpha = 0 \\ (-\Lambda\alpha s + 1)^{-\frac{1}{\alpha}} & \text{otherwise.} \end{cases} \quad (2)$$

We call Eq. (2) the *intrinsic curvature function* because every point of a curve can be related to Eq. (2) in terms of α computed in Section 3. Eq. (2) is slightly different from the equation in [13] since the curvature is assumed to be monotonically increasing. As demonstrated in [14], log-aesthetic curves do not change their shape depending on the value of Λ except when $\alpha = 1$. In other words, the value of Λ changes the shape of the curve only when $\alpha = 1$, which is the case of logarithmic spirals. Fig. 1 shows the curvature plot of log-aesthetic curves in the standard form with $\Lambda = 1$ and $\alpha = -2, -1, 0, 1$, and 2 .

Fig. 2 shows the curvature plot, the curvature comb, and the LCG of a cubic Bézier curve with monotonically varying curvature. The curve is shown in Fig. 2 (b). The endpoints a, b of the curve correspond to a, b in Fig. 2 (a) and (c), but which point of a curve corresponds to which point in the LCG is not clear. Fig. 3 shows the same plots of a cubic Bézier curve with the curvature maximum and minimum. At the curvature

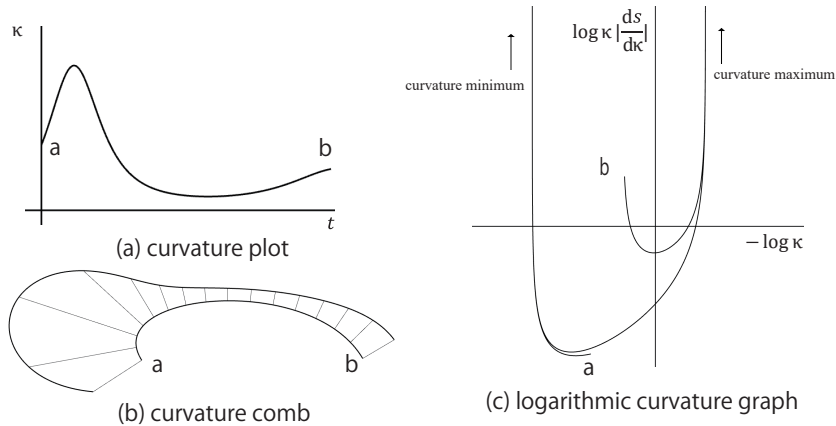


Figure 3: Cubic Bézier curve with curvature extrema.

extrema, $\log\left(\kappa \frac{ds}{d\kappa}\right)$ becomes infinite since $\frac{d\kappa}{ds} = 0$. The LCG slope α becomes $-\infty$ at curvature minima and ∞ at curvature maxima. Again, understanding which point of the curve corresponds to which point in the LCG is not easy.

For space curves, let τ be the torsion. The linearity of LTG is

$$\log\left(\tau \frac{ds}{d\tau}\right) = -\beta \log \tau + d. \quad (3)$$

The torsion function in the standard form ($\tau = 1$ at $s = 0$) is, by setting $\Omega = e^{-d}$,

$$\tau = \begin{cases} e^{\Omega s} & \text{if } \beta = 0 \\ (-\Omega\beta s + 1)^{-\frac{1}{\beta}} & \text{otherwise.} \end{cases} \quad (4)$$

We call Eq. (4) the *intrinsic torsion function*. The properties of LTGs are similar to LCGs by replacing κ and α with τ and β , respectively.

3 SHAPE INFORMATION REGARDING THE SLOPES OF LCGS AND LTGS

In this section, we derive an equation for the slope α of the LCG in terms of curvature. The slope β of the LTGs in terms of torsion is similarly derived. Gobithaasan et al. derived the equation for the slopes of LCGs in terms of the radius of curvature [5]. We derive the slopes of LCG by curvature and describe detail properties such as the case $\frac{d\kappa}{ds}$ is zero or negative. We also derive the equation for the slopes of LTGs.

The slope of LCG α is

$$\alpha = -\frac{d \log\left(\kappa \frac{ds}{d\kappa}\right)}{d \log \kappa} \quad (5)$$

$$\begin{aligned} &= -\frac{d \log\left(\kappa \frac{ds}{d\kappa}\right)}{d\kappa} \frac{d\kappa}{d \log \kappa} = -\frac{\frac{ds}{d\kappa} + \kappa \frac{d^2s}{d\kappa^2}}{\kappa \frac{ds}{d\kappa}} \kappa = -1 - \kappa \frac{d^2s}{d\kappa^2} \frac{d\kappa}{ds} \\ &= -1 + \kappa \frac{d^2\kappa}{ds^2} / \left(\frac{d\kappa}{ds}\right)^2. \end{aligned} \quad (6)$$

The value of α does not depend on the position, rotation, and scaling of a curve. Of course, the curvature and the arc length are independent of the position and rotation. Scaling the curvature function by s means scaling the curve by $\frac{1}{s}$. Scaling the curvature function by s also scales $\frac{d\kappa}{ds}$ and $\frac{d^2\kappa}{ds^2}$ by s . Therefore, the value of α does not change by scaling.

Eq. (6) works well when $\kappa < 0$ and/or $\frac{d\kappa}{ds} < 0$. If $\kappa < 0$, κ in Eq. (5) is replaced by $-\kappa$. If $\frac{d\kappa}{ds} < 0$, $\frac{d\kappa}{ds}$ in Eq. (5) is replaced by $-\frac{d\kappa}{ds}$. In all these cases, the same Eq. (6) can be derived. If the value of α is α_p at a point of the curve, it means that the curve can be best approximated with the log-aesthetic curve of $\alpha = \alpha_p$ at the point. In other words, the curvature can be best approximated with the intrinsic curvature function of $\alpha = \alpha_p$ at the point.

α is not defined if $\frac{d\kappa}{ds} = 0$ or $\kappa = \infty$. Therefore, α is not defined at any point of a circular arc, curvature extrema, or cusps. α may not be defined at an inflection point when $\frac{d\kappa}{ds} = 0$ or $\frac{d\kappa}{ds}$ is indeterminate. In such situations, we can still compute α at an inflection point by taking the limit of α as the parameter t approaches the value of the inflection point.

In the implementation, if $\frac{d\kappa}{ds} = 0$ at a certain point of a curve, the nearby value of α can be used by sufficiently sampling the points on the curve. For a circular arc, very large value of α may be used since taking the limit of Eq. (2) as α approaches $\pm\infty$, we get a circle ($\kappa = 1$).

The derivation of the LTG slope is similar. By replacing α and κ in Eq. (5) with β and τ , respectively, we can derive the following equation.

$$\beta = -1 + \tau \frac{d^2\tau}{ds^2} / \left(\frac{d\tau}{ds} \right)^2. \quad (7)$$

Similarly as in α , β does not depend on the position, rotation and scaling of the curve. Eq. (7) works well when $\frac{d\tau}{ds} < 0$. β is not defined when $\frac{d\tau}{ds} = 0$. Therefore, β is not defined for curves with a constant torsion, such as planar curves and a helix. β is not also defined at torsion extrema.

By computing α (and β for space curves), we can obtain the shape information of curves related to log-aesthetic (space) curves. The shape information is independent of the position, rotation, and scaling of the curves. The value of α or β tells us that the curvature or torsion function is best approximated by the intrinsic curvature or torsion function. In Appendix A, we show the Mathematica code for computing the LCG slope of the hyperbolic spiral.

4 VISUALIZING THE SHAPE INFORMATION USING TWO-TONE PSEUDO COLORING

In this section, we visualize the shape information using the two-tone pseudo coloring [11] proposed by Saito et al. In the two-tone pseudo coloring, a user can read out approximate values from the colors of the paint.

Fig. 4 shows the comparison of continuous coloring and two-tone pseudo coloring. In both the coloring methods, the color is gray at $\alpha = 0$ and red at $\alpha = 1$. In continuous coloring, the color changes continuously by linearly interpolating the color from gray to red. In two-tone pseudo coloring, as the value α changes from 0 to 1, the height of the color changes. For example, if the height of the red color is approximately $\frac{1}{3}$ of the total height and the other color is gray, we can read out the approximate value as $\alpha = \frac{1}{3}$. See Fig. 4 (b). In contrast, in continuous coloring shown in Fig. 4 (a), it is not easy to read out the approximate value from interpolated colors because the human eye's color perception is affected by nearby colors, making it difficult to correctly distinguish subtle differences. Note that, in two-tone pseudo coloring, if the upper one-third of the total height of the coloring is red and the lower two-thirds is gray, we can still read out the approximate value as $\frac{1}{3}$. Therefore, we can read out the approximate value when color inversion between top and bottom occurs. For parametrization independent two-tone pseudo coloring of curves, the color inversion occurs at an inflection point. More details on two-tone pseudo coloring are described in [11].

In this work, we set the colors of two-tone coloring blue, gray, red, and orange when $\alpha = -1, 0, 1$ and 2 , respectively. These values of α are particularly meaningful because the curve becomes the Clothoid, Nielsen's

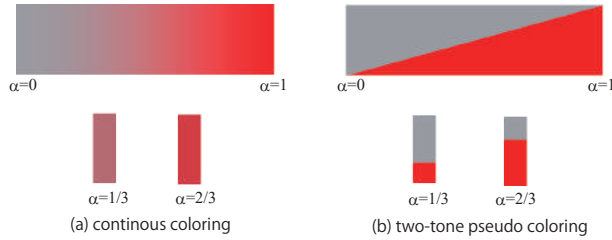


Figure 4: Comparison of continuous coloring and two-tone pseudo coloring.

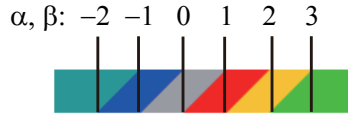


Figure 5: Two-tone pseudo coloring and the values of α and β .

spiral, a logarithmic spiral, or the circle involute corresponding to these values of α . Warm colors are used for positive α , whereas cold colors are used for negative α . For $\alpha = 0$, gray, the achromatic color, is used. The color is dark cyan when α is less than -2 or green when α is greater than 3 . The same coloring is used for β . See Fig. 5.

Fig. 6 compares continuous coloring and two-tone pseudo coloring applied to the same curve. In two-tone pseudo coloring, the approximate value for each point of the curve, as well as the speed of the change of the value, is more easily readable.

Fig. 7 shows the various visualizations of the shape information (α) of planar curves. The shape information is shown on the curve, on the curvature comb or on the curvature plot in Fig. 7 (a), (b) or (c), respectively. For planar curves, we show the shape information on the curve in this paper. In case the shape information should not be shown on the curve, it may be shown on the curvature comb or the curvature plot. For space curves, the LCG slope α and the LTG slope β are shown on the curvature comb and the torsion comb, respectively. See Fig. 14 for example. Note that for thicker line width, approximate values can be easier to read out, but the curve shape becomes more ambiguous. In our application, the line width can be changeable. Therefore, a user can change the line width when necessary, such as the case thicker line is preferable.

Fig. 8 shows the parametrization dependent and independent visualization of the shape information on the curve. In Fig. 8 (a),(b) and (c), the arrows show the upward direction of two-tone pseudo coloring. In Fig. 8 (a) and (b), for the upward direction of two-tone pseudo coloring, the tangent of the curve rotated counter-clockwise by $\frac{\pi}{2}$ is used. Since the order of control points is flipped, the parametrization of these curves is different. Looking at the coloring, the colors are inversely painted between up and bottom. Therefore, if we use the rotated tangent of the curve, the visualization is parametrization dependent. In Fig. 8 (c) and (d), the

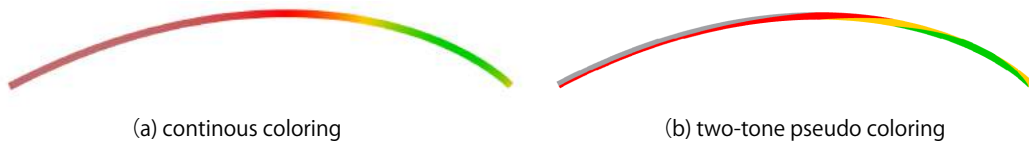


Figure 6: Coloring comparison of the same curve.

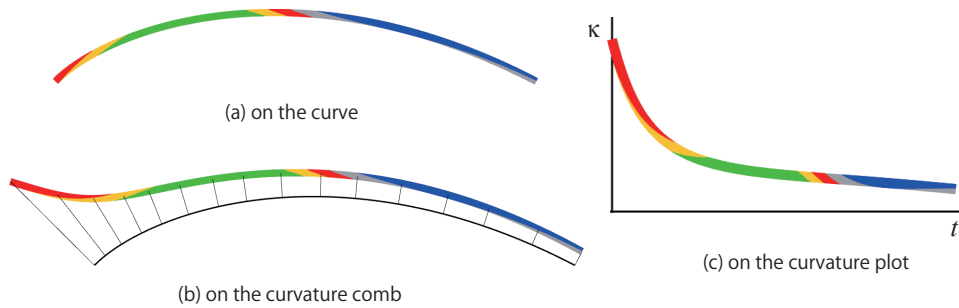


Figure 7: Various visualization of shape information.

normal of the curve is used for the height of the two-tone pseudo coloring. The colorization is parametrization independent; thus changing the order of control points does not change the colorization. However, color inversion occurs at an inflection point. In most polynomial curves, it is known that α gets closer to -1 near the inflection point [13]. At the inflection point in Fig. 8 (c), we do not recognize the color inversion since only the blue color is used. Looking at the coloring at the inflection point in Fig. 8 (d), gray and blue colors are used near the inflection point and color inversion occurs at the inflection point. Note that the inflection point occurs at $t = \frac{1}{2}$ and α is not defined at the point. However, if we take the limit of α as t approaches $\frac{1}{2}$, α becomes $\frac{1}{3}$. Color inversion does not occur if we use the rotated tangents, though the coloring is parametrization dependent. In this paper, we use colorization using normals when we show on the shape information on the curve so that the coloring becomes parametrization independent.

Fig. 9 shows the visualization of α of a polynomial quadratic Bézier curve which is a parabola. The slope of the LCG of a parabola approaches $\frac{2}{3}$ when it is farther away from the vertex of the parabola [9]. This fact can be confirmed in Fig. 9 since the slope gets closer to $\frac{2}{3}$ as the curve point gets farther away from the vertex of the parabola.

Fig. 10 (a) shows a polynomial cubic Bézier curves with a curvature maximum. The color becomes dark cyan near curvature maxima. Fig. 10 (b) shows a polynomial cubic Bézier curves with a curvature minimum. The color becomes green near curvature minima.

Fig. 11 is an example of a cubic Bézier curve that is close to a logarithmic spiral. The control points are manually placed so that the curve gets closer to a logarithmic spiral ($\alpha = 1$). Initially, the control points are placed so that they roughly satisfy the condition of typical Bézier curves [3], which are known to get closer to logarithmic spirals as the degree gets higher. In typical Bézier curves, $\frac{|\mathbf{P}_{i+2} - \mathbf{P}_{i+1}|}{|\mathbf{P}_{i+1} - \mathbf{P}_i|}$ is a constant and the angle between $\mathbf{P}_{i+1} - \mathbf{P}_i$ and $\mathbf{P}_{i+2} - \mathbf{P}_{i+1}$ is also a constant. Then the control points are fine-tuned so that the coloring approaches single red color. Manually finding the placement of control points is relatively easy for $\alpha = 1$. For other α , finding the placement of control points is not easy since the geometric property like typical Bézier curves are not known.

Fig. 12 shows examples of rational cubic Bézier curves optimized for $\alpha = -1, -0.5, 0, 0.5, 1, 1.5$ and 2 with the same G^1 Hermite interpolation condition. Note that, for example, when $\alpha = 2$, the coloring is not single yellow because rational cubic Bézier curves cannot exactly represent log-aesthetic curves.

Fig. 13 (a) shows a rational cubic Bézier curve close to a circular arc. Its curvature plot is shown in Fig. 13 (b). The curvature seems to be constant, but it actually is not. Visualization of the shape information of curves whose curvature (and torsion for space curves) is nearly a constant may be meaningless since a very small change of curvature changes the value of α .

Fig. 14 (a) is an example of space curves, where α and β are shown on the curvature comb and torsion comb, respectively. Similarly, as in the case of curvature, if the coloring of a portion of the torsion comb is

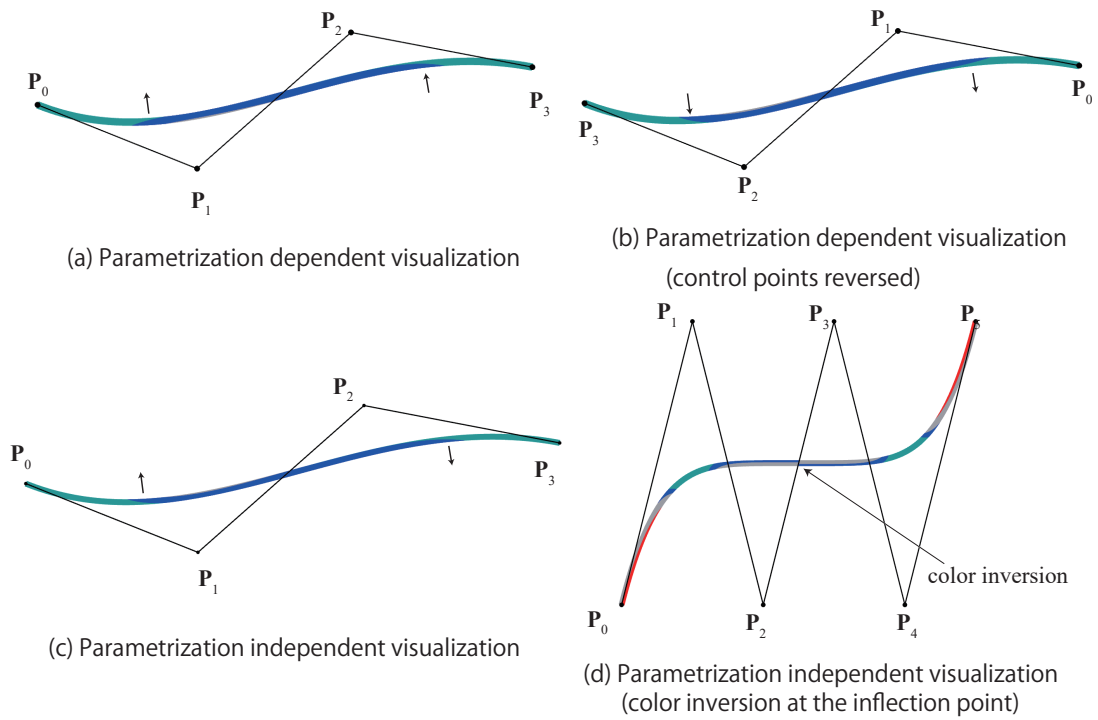


Figure 8: Parametrization dependent/independent visualization using two-tone pseudo coloring.

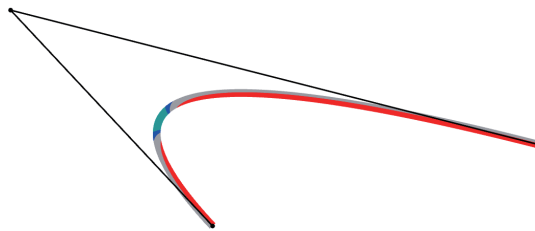


Figure 9: Polynomial quadratic Bézier curve.

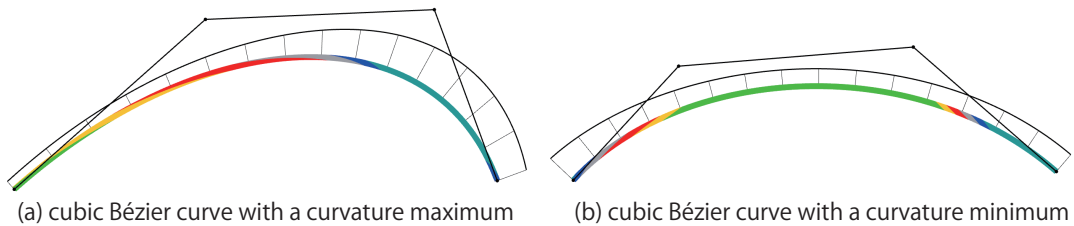


Figure 10: Polynomial cubic Bézier curves with curvature extrema.

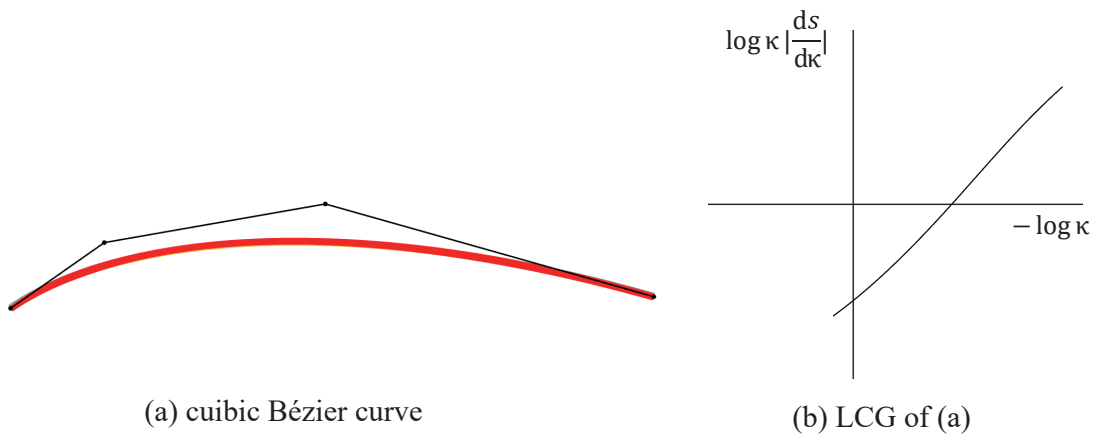


Figure 11: Cubic Bézier curve close to a logarithmic spiral and its LCG.

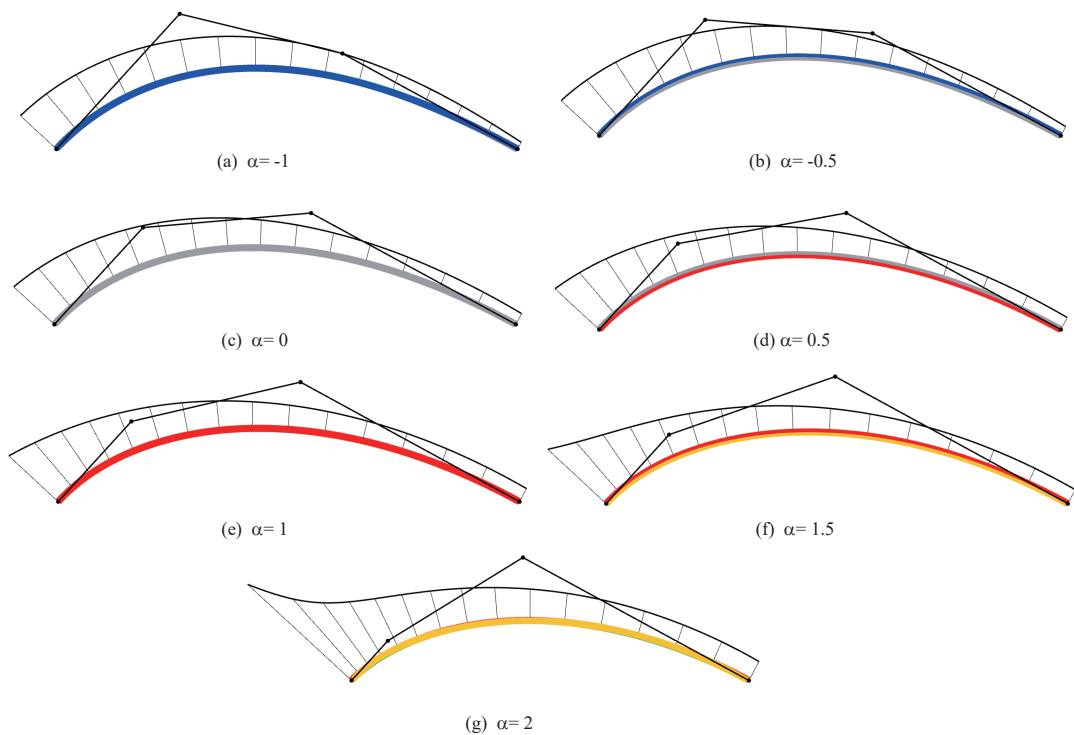


Figure 12: Rational cubic Bézier curves optimized for specific α .

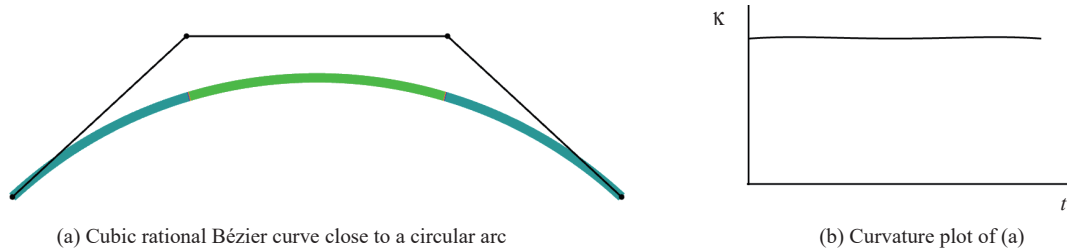


Figure 13: Rational cubic Bézier curve close to a circular arc.

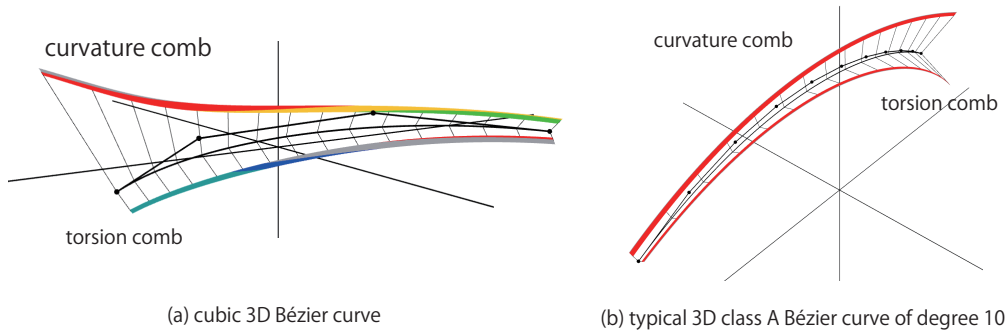


Figure 14: 3D polynomial cubic Bézier curves.

almost red, we can obtain the information that the torsion function is close to the case of $\beta = 1$, which means the torsion is close to be inversely proportional to the arc length. Fig. 14 (b) is a typical 3D class A Bézier curve [3] of degree 10. Under the same G^1 Hermite condition, it is known that typical 3D class A Bézier curves get closer to the 3D extension of logarithmic spirals ($\alpha = 1$ and $\beta = 1$) as the degree gets higher [13]. Therefore, the coloring of α and β is both close to be single red. The space curve with $\alpha = 1$ and $\beta = 1$ is a 3D logarithmic spiral, and the curve $\alpha = -1$ and $\beta = -1$ is the 3D Clothoid curve. By visualizing the shape information of space curves, we can see the similarity to these curves.

5 SHAPE ANALYSIS OF PLANAR CURVES USING THE LCG SLOPE

In this section, we investigate the shape similarities of some planar curves with log-aesthetic curves by computing the LCG slopes. We picked up planar curves in differential geometry [6] that have similarities with log-aesthetic curves. Although the planar curves in this section are well-known, the similarities to log-aesthetic curves are not known.

We denote the LCG slope at parameter t as $\alpha(t)$. By taking the limit of $\alpha(t)$ as t approaches the limit value, such as $\pm\infty$, we clarify the similarities to log-aesthetic curves. For each planar curve, we indicate the approximate parameter values of t where the value of α gets within ± 0.01 of the limit α .

[Lituus]

The equation of a lituus is

$$\text{lituus}(t) = \left[\frac{a \cos(t)}{\sqrt{t}} \quad \frac{a \sin(t)}{\sqrt{t}} \right]^T \quad (t > 0). \tag{8}$$

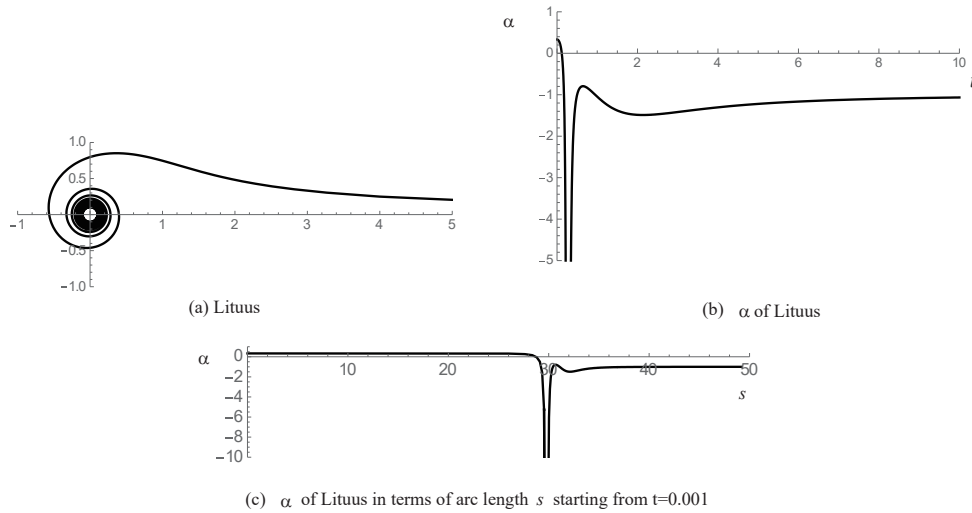


Figure 15: Lituus and its LCG slope.

The LCG slope of the lituus is, without depending on a ,

$$\alpha_{\text{lituus}}(t) = \frac{3 - 32t^2 (8t^6 + 96t^4 - 19t^2 + 7)}{(16t^4 + 40t^2 - 3)^2}. \quad (9)$$

Without depending on a , the lituus has a local curvature maximum at $t = \sqrt{\frac{\sqrt{7}}{2} - \frac{5}{4}} (\approx 0.269955)$ and an inflection point at $t = \frac{1}{2}$. Therefore, $\alpha_{\text{lituus}}(t)$ becomes $-\infty$ at the point of curvature maximum. $\alpha_{\text{lituus}}(t)$ is not defined at the inflection point, but the limit of $\alpha_{\text{lituus}}(t)$ is -1 as t approaches $\frac{1}{2}$.

The limit of $\alpha_{\text{lituus}}(t)$ as t approaches ∞ is -1 . Thus, the circular-like part of the lituus gets similar to the Clothoid ($\alpha = -1$) as t gets larger. The limit of $\alpha_{\text{lituus}}(t)$ as t approaches 0 is $\frac{1}{3}$. The region of α close to $\frac{1}{3}$ in terms of parameter t is very small as shown in Fig. 15 (b). But as t approaches 0, x coordinates can be arbitrarily large. Fig. 15 (c) shows the LCG slope with respect to the arc length measured from $t = 0.0001$ with $a = 1$. The region of the lituus with $\alpha \approx \frac{1}{3}$ is infinitely large. At $t = 0.028$ or 27 , $\alpha_{\text{lituus}}(t)$ is approximately 0.32053 or -1.00952 , respectively.

[Hyperbolic spiral]

The equation of a hyperbolic spiral is

$$\text{hyperbolic}(t) = \left[a \frac{\cos t}{t} \quad a \frac{\sin t}{t} \right]^T \quad (t > 0). \quad (10)$$

The LCG slope of the hyperbolic spiral is, without depending on a ,

$$\alpha_{\text{hyperbolic}}(t) = \frac{4 - 5t^2}{(t^2 + 4)^2}. \quad (11)$$

As t approaches ∞ , the limit of $\alpha_{\text{hyperbolic}}(t)$ is 0. Thus, the circular-like part of the hyperbolic spiral gets closer to the log-aesthetic curve of $\alpha = 0$ as t gets larger. The limit of $\alpha_{\text{hyperbolic}}(t)$ as t approaches 0 is $\frac{1}{4}$. Thus, the hyperbolic spiral gets closer to the log-aesthetic curve of $\alpha = \frac{1}{4}$ as t approaches to 0. The region of

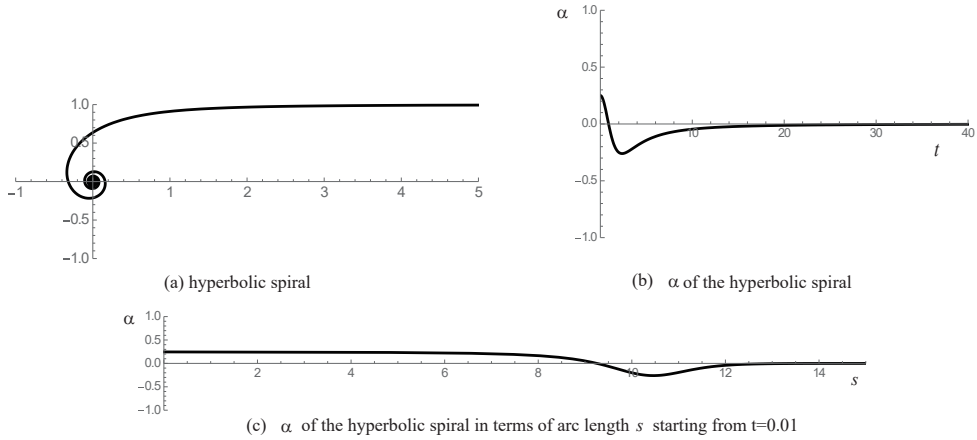


Figure 16: Hyperbolic spiral and its LCG slope.

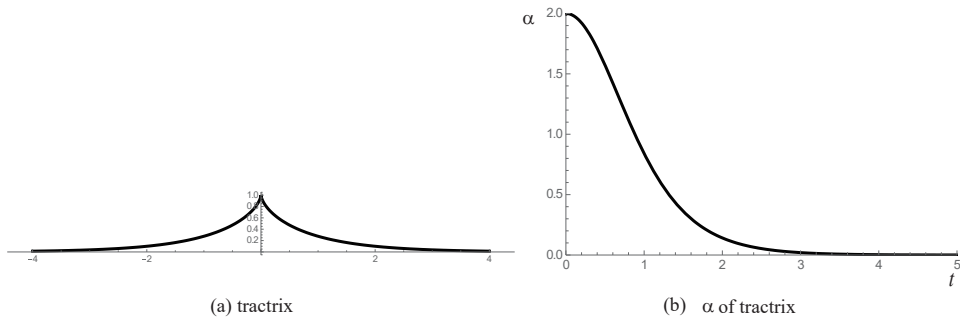


Figure 17: Tractrix and its LCG slope.

parameter t where the hyperbolic parabola is closer to $\alpha = \frac{1}{4}$ is very small, but its actual region with respect to the arc length can be arbitrarily large. See Fig. 16.

[Tractrix]

The equation of a tractrix is

$$\text{tractrix}(t) = [t - \tanh(t), a \operatorname{sech}(t)]^T. \tag{12}$$

The LCG slope of the tractrix is

$$\alpha_{\text{tractrix}}(t) = \frac{-2(16a^4 - 103a^2 + 57) \cosh(2t) + 4(4a^4 + 5a^2 - 3) \cosh(4t) + 2(9 - 7a^2) \cosh(6t) + 4(36a^4 - 53a^2 + 27)}{\left((12 - 8a^2) \cosh(2t) + 16a^2 + \cosh(4t) - 13 \right)^2}. \tag{13}$$

Computing the limit of $\alpha_{\text{tractrix}}(t)$ as $t \rightarrow 0$ or $t \rightarrow \infty$, we get $\alpha = 2$ or $\alpha = 0$ without depending on a . See Fig. 17. The region of the curve close to $\alpha = 2$ is very small. At $t = 3.4$, $\alpha_{\text{tractrix}}(t)$ is approximately 0.00889039.

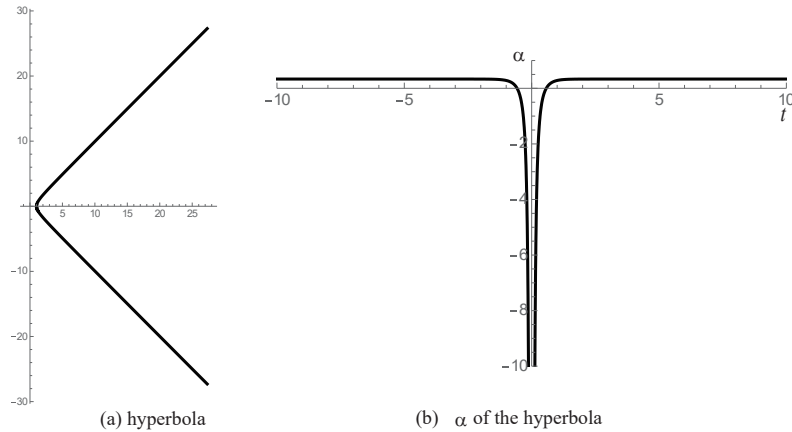


Figure 18: Hyperbola and its LCG slope.

[Hyperbola]

The equation of a hyperbola is

$$\mathbf{hyperbola}(t) = [a \cosh(t) \quad a \sinh(t)]^T. \quad (14)$$

The LCG slope of the hyperbola is, without depending on a ,

$$\alpha_{\text{hyperbola}}(t) = \frac{1}{24}(\cosh(4t) - 5)\text{csch}^2(t)\text{sech}^2(t). \quad (15)$$

Taking the limit of $\alpha_{\text{hyperbola}}(t)$ as t approaches $\pm\infty$, we get $\alpha = \frac{1}{3}$. See Fig. 18. At $t = \pm 1.67178$, $\alpha_{\text{hyperbola}}(t)$ is approximately 0.33.

[Cissoid of Diocles]

The equation of Cissoid of Diocles is

$$\mathbf{Cissoid}(t) = \left[\frac{2at^2}{t^2 + 1} \quad \frac{2at^3}{t^2 + 1} \right]^T. \quad (16)$$

The LCG slope of Cissoid of Diocles is

$$\alpha_{\text{Cissoid}}(t) = \frac{t^4 - 3t^2 + 8}{4(t^2 + 1)^2}. \quad (17)$$

Computing the limit of Eq. (17) as $t \rightarrow 0$ or $t \rightarrow \infty$, we get $\alpha = 2$ or $\alpha = \frac{1}{4}$. See Fig. 19. The region of the curve close to $\alpha = 2$ is very small. At $t = 11.1$, $\alpha_{\text{Cissoid}}(t)$ is approximately 0.240131.

[Spiral of Archimedes]

The equation of the spiral of Archimedes is

$$\mathbf{Archimedes}(t) = [at \cos t \quad at \sin t]^T \quad (t \geq 0). \quad (18)$$

The LCG slope of the spiral of Archimedes is, without depending on a ,

$$\alpha_{\text{Archimedes}}(t) = \frac{2t^6 + 15t^4 + 14t^2 - 8}{t^2(t^2 + 4)^2}. \quad (19)$$

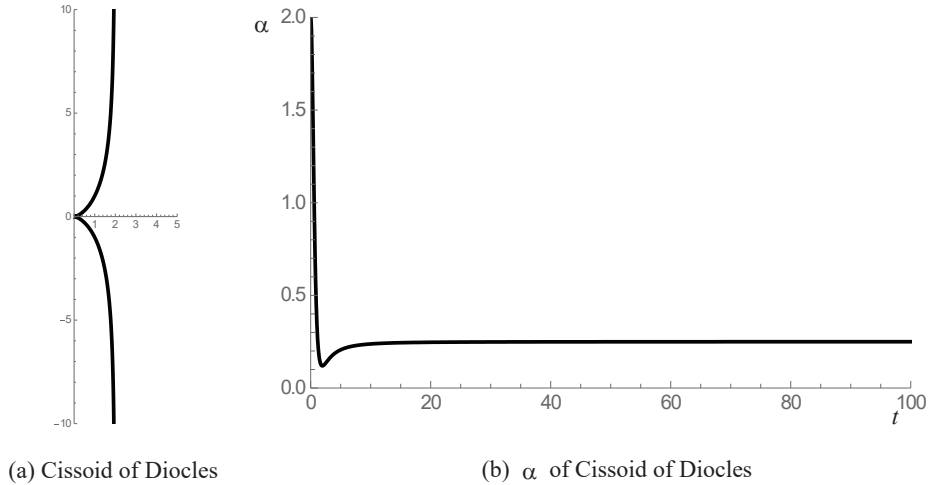


Figure 19: Cissoid of Diocles and its LCG slope.

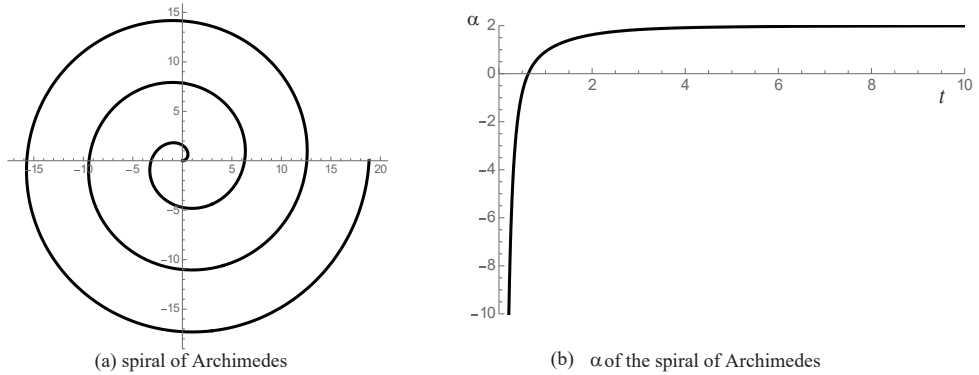


Figure 20: The spiral of Archimedes and its LCG slope.

Taking the limit of Eq. (19) as t approaches ∞ , we get $\alpha = 2$. Thus as t gets larger, the spiral of Archimedes gets closer to the circle involute, which is the log-aesthetic curve of $\alpha = 2$. See Fig. 20. At $t = 10.5$, $\alpha_{\text{Archimedes}}(t)$ is approximately 1.99017.

[Fermat’s spiral]

The equation of Fermat’s spiral is

$$\mathbf{Fermat}(t) = \left[a\sqrt{t} \cos t \quad a\sqrt{t} \sin t \right]^T. \tag{20}$$

The LCG slope of Fermat’s spiral is, without depending on a ,

$$\alpha_{\text{Fermat}}(t) = \frac{32t^2 (24t^6 + 128t^4 + 23t^2 - 21) - 9}{(16t^4 + 40t^2 - 3)^2}. \tag{21}$$

Fermat’s spiral has a curvature maximum at $t = \sqrt{\frac{\sqrt{7}}{2} - \frac{5}{4}} \approx 0.269955$ without depending on a , and the LCG

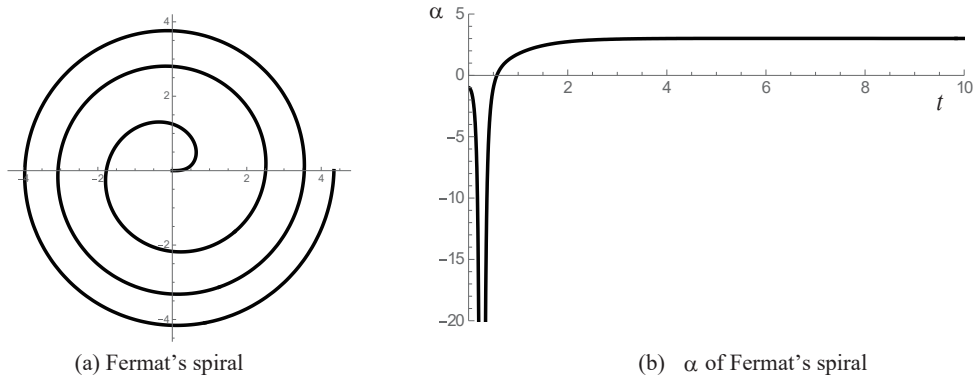


Figure 21: Fermat's spiral and its LCG slope.

slope become $-\infty$ at the curvature maximum. By taking the limit of $\alpha_{\text{Fermat}}(t)$ as t approaches ∞ , we get $\alpha = 3$. Therefore, Fermat's spiral gets closer to the log-aesthetic curve of $\alpha = 3$ as t gets larger. See Fig. 21. At $t = 3.6$, $\alpha_{\text{Fermat}}(t)$ is approximately 2.99255.

Fig. 22 shows the visualization of the shape information of the curves in this section and the similarities with log-aesthetic curves. For example, both the lituus and the hyperbolic spiral get closer to circular arcs near the origin, but their LCG slopes are different. Since α of the lituus gets closer to -1 , it means that the curvature function near the origin is close to be linear with respect to arc length. For the hyperbolic spiral, the curvature function near the origin is close to an exponential function since α gets close to 0.

As t of the lituus gets closer to 0 and as t of the hyperbola or Cissoid of Diocles gets closer to $\pm\infty$, all the LCG slopes of these curves get closer to $\frac{1}{3}$. Therefore, these curves have similar regions close to the log-aesthetic curve of $\alpha = \frac{1}{3}$. The spiral of Archimedes is close to the log-aesthetic curve of $\alpha = 2$ except for the region near the origin. Only in Fermat's spiral, the extended two-tone pseudo coloring shown in (h) is used. In the extended two-tone-pseudo coloring, the color of $\alpha = 3$ is added because α of Fermat's spiral gets closer to 3 as the parameter t increases.

6 CONCLUSIONS

In this paper, we derived the LCG slope α and the LTG slope β of curves in terms of curvature and torsion. By computing α and β for each point of a differentiable parametric curve, we can get the shape information related to log-aesthetic (space) curves. We also proposed a method for visualizing the shape information using two-tone pseudo coloring. By using two-tone pseudo coloring, users can read out the approximate value of α or β for each point of a curve. For some planar parametric curves in differential geometry, we clarified the similarities with log-aesthetic curves by taking the limit of α as the parameter t approaches the limit value. For example, in the lituus, the hyperbola, and Cissoid of Diocles, there are similar regions with the log-aesthetic curve of $\alpha = \frac{1}{3}$.

Future work includes clarifying the similarities of spaces curves with log-aesthetic space curves and extending the visualization of shape information to surfaces.

A MATHEMATICA CODE FOR COMPUTING THE LCG SLOPE

Mathematica Code 1 shows a code for computing the LCG slope of the hyperbolic spiral. By replacing `HyperbolicSpiral[a_][t_]`, we can compute the LCG slopes of other curves, including Bézier curves or B-

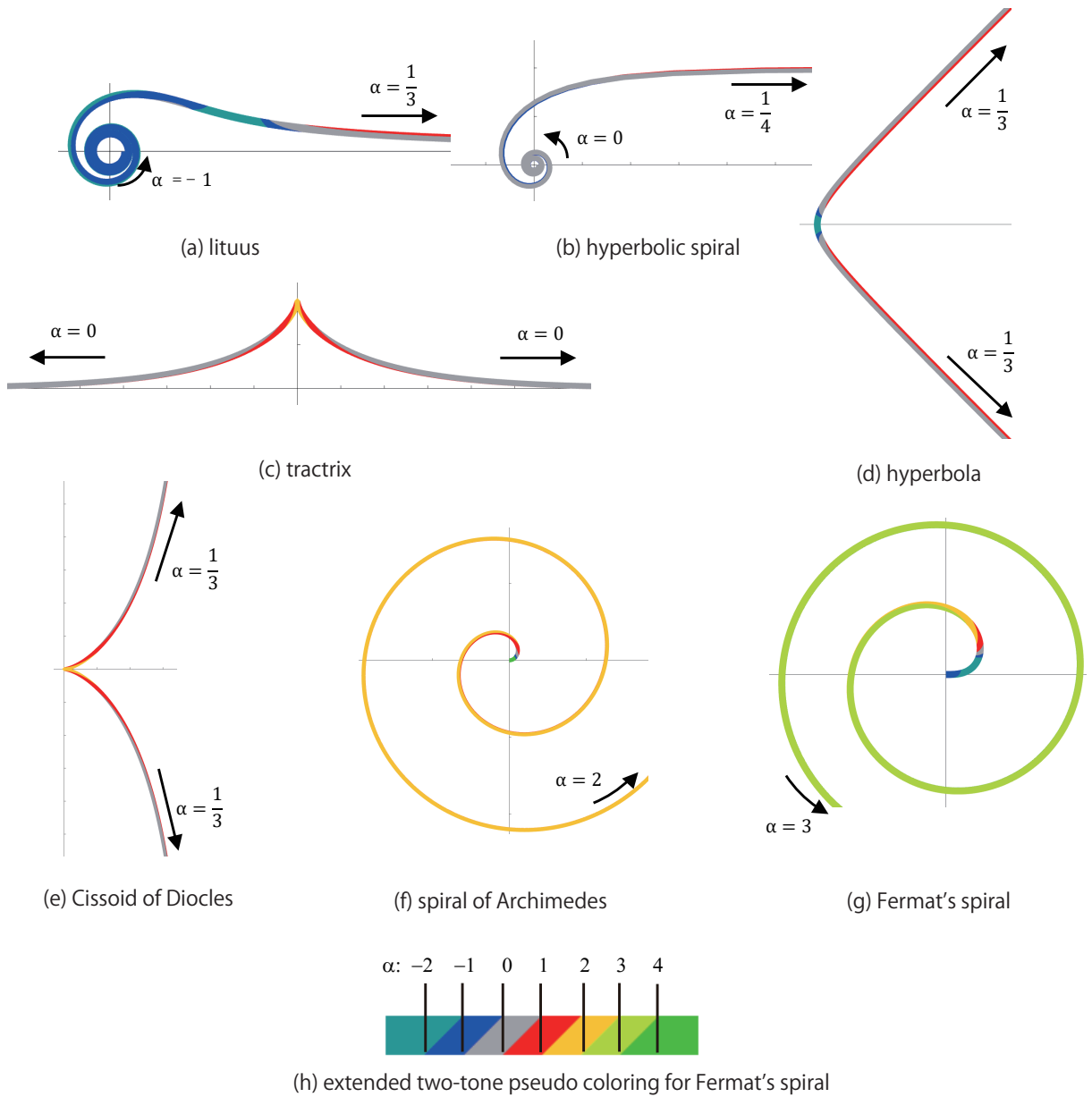


Figure 22: Two-tone pseudo coloring of the shape information of various planer curves.

spline curves, either polynomial or rational. We can also compute the LTG slope by replacing the curvature function with the torsion function.

Mathematica Code 1: Computing the LCG slope of the Hyperbolic Spiral

```
In[1]:= normfd[f_][t_] :=
Sqrt[D[f[x], x] . D[f[x], x]] /. x -> t

In[2]:= kappa[f_][t_] :=
Sqrt[Cross[D[f[x], {x, 1}], D[f[x], {x, 2}]] .
Cross[D[f[x], {x, 1}], D[f[x], {x, 2}]]]
/normfd[f][x]^3 /. x -> t

In[3]:= dkds[f_][t_] :=
D[kappa[f][x], x]/normfd[f][x] /. x -> t

In[4]:= d2kds2[f_][t_] :=
D[kappa[f][x], {x, 2}]/normfd[f][x]^2 -
D[kappa[f][x], x] D[f[x], x] . D[f[x], {x, 2}]
/normfd[f][x]^4 /. x -> t

In[5]:= lcgSlope[f_][t_] :=
-1 + kappa[f][x] d2kds2[f][x]/(dkds[f][x]^2) /. x -> t

In[6]:= HyperbolicSpiral[a_][t_] :=
{a Cos[t]/t, a Sin[t]/t, 0}

In[7]:= lcgSlope[HyperbolicSpiral[a]][t] // FullSimplify

Out[7]= (4 - 5 t^2)/(4 + t^2)^2
```

ACKNOWLEDGEMENTS

The authors would like to express their gratitude to anonymous reviewers for their valuable comments.

Norimasa Yoshida, <http://orcid.org/0000-0001-8889-0949>

Takafumi Saito, <http://orcid.org/0000-0001-5831-596X>

REFERENCES

- [1] Dill, J.C.: An application of color graphics to the display of surface curvature. SIGGRAPH '81: Proceedings of the 8th annual conference on Computer graphics and interactive techniques, 153–161, 1981. <http://doi.org/10.1145/800224.806801>.
- [2] Farin, G.: Curves and Surfaces for Computer Aided Geometric Design, 5th ed. Morgan-Kaufmann, 2001.
- [3] Farin, G.: Class A Bézier curves. Computer Aided Geometric Design, 23(7), 573–581, 2006. <http://doi.org/10.1016/j.cagd.2006.03.004>.
- [4] Farin, G.: Curvature combs and curvature plots. Computer-Aided Design, 80, 6–8, 2016. <http://doi.org/10.1016/j.cad.2016.08.003>.

- [5] Gobithaasan, R.U.; Miura, K.T.: Logarithmic curvature graph as a shape interrogation tool. *Applied Mathematical Science*, 8(16), 755–765, 2014. <http://doi.org/10.12988/ams.2014.312709>.
- [6] Gray, A.; Abbena, E.; Salamon, S.: *Modern Differential Geometry of Curves and Surfaces with MATHEMATICA*, Third Edition. Chapman & Hall/CRC, 2006.
- [7] Harada, T.; Yoshimoto, F.; Moriyama, M.: An aesthetic curve in the field of industrial design. In *Proceedings of IEEE Symposium on Visual Languages*, 38–47, 1999. <http://doi.org/10.1109/VL.1999.795873>.
- [8] Klass, R.: Correction of local surface irregularities using reflection lines. *Computer-Aided Design*, 12(2), 73–77, 1980. [http://doi.org/10.1016/0010-4485\(80\)90447-9](http://doi.org/10.1016/0010-4485(80)90447-9).
- [9] Miura, K.T.: A general equation of aesthetic curves and its self-affinity. *Computer Aided Design and Applications*, 3(1-4), 457–464, 2006. <http://doi.org/10.1080/16864360.2006.10738484>.
- [10] Poeschl, T.: Detecting surface irregularities using isophotes. *Computer Aided Geometric Design*, 1(2), 163–168, 1984. [http://doi.org/10.1016/0167-8396\(84\)90028-1](http://doi.org/10.1016/0167-8396(84)90028-1).
- [11] Saito, T.; Miyamura, H.; Yamamoto, M.; Saito, H.; Hoshiya, Y.; Kaseda, T.: Two-tone pseudo coloring: compact visualization for one-dimensional data. In *IEEE Symposium on Information Visualization*, 2005. *INFOVIS 2005.*, 173–180, 2005. <http://doi.org/10.1109/INFVIS.2005.1532144>.
- [12] Yoshida, N.; Fukuda, R.; Saito, T.: Log-aesthetic space curve segments. In *SIAM/ACM Joint Conference on Geometric and Physical Modeling*, 35–46, 2009. <http://doi.org/10.1145/1629255.1629261>.
- [13] Yoshida, N.; Fukuda, R.; Saito, T.: Logarithmic curvature and torsion graphs. In *Mathematical Methods for Curves and Surfaces (MMCS 2008)*, *Lecture Notes in Computer Science (LNCS 5862)*, 434–443, 2010. http://doi.org/10.1007/978-3-642-11620-9_28.
- [14] Yoshida, N.; Saito, T.: Interactive aesthetic curve segments. *The Visual Computer (Pacific Graphics)*, 22(9–11), 896–905, 2006. <http://doi.org/10.1007/s00371-006-0076-5>.
- [15] Yoshida, N.; Saito, T.: Quadratic log-aesthetic curves. *Computer Aided Design and Applications*, 14(2), 219–226, 2017. <http://doi.org/doi.org/10.1080/16864360.2016.1223434>.
- [16] Ziatdinov, R.; Yoshida, N.; Kim, T.: Analytic parametric equations of log-aesthetic curves in terms of incomplete gamma functions. *Computer Aided Geometric Design*, 29(2), 129–140, 2012. <http://doi.org/10.1016/j.cagd.2011.11.003>.